Available online at www.sciencedirect.com
ScienceDirect
Lithos 104 (2008) 216–230
LITHOS
www.elsevier.com/locate/lithos

Geochemistry and Nd–Sr isotopic studies of Late Mesozoic granitoids in the southeastern Hubei Province, Middle–Lower Yangtze River belt, Eastern China: Petrogenesis and tectonic setting

Guiqing Xie [a,b,c,*], Jingwen Mao [c], Ruiling Li [d], Frank P. Bierlein [e]

[a] State Key Laboratory of Geological Process and Mineral Recourse, China University of Geosciences, Beijing, 100083, China
[b] Institute of Mineral Resources, Chinese Academy of Geological Sciences, Beijing, 100037, China
[c] State Key Laboratory of Ore Deposit Geochemistry, Institute of Geochemistry, Chinese Academy of Sciences, Guiyang, 550002, China
[d] Development of Geological and Research Center, China Geological Surveys, Beijing, 100037, China
[e] Centre for Exploration Targeting and Tectonics Research Centre, School of Earth and Geographical Sciences, University of Western Australia, Crawley, WA 6009, Australia

Received 20 April 2007; accepted 21 December 2007
Available online 16 January 2008

Abstract

A geochemical and isotopic study was carried out for the Mesozoic Yangxin, Tieshan and Echeng granitoid batholiths in the southeastern Hubei Province, eastern China, in order to constrain their petrogenesis and tectonic setting. These granitoids dominantly consist of quartz diorite, monzonite and granite. They are characterized by SiO_2 and Na_2O compositions of between 54.6 and 76.6 wt.%, and 2.9 to 5.6 wt.%, respectively, enrichment in light rare earth elements (LREE) and large ion lithophile elements (LILE), and relative depletion in Y (concentrations ranging from 5.17 to 29.3 ppm) and Yb (0.34–2.83 ppm), with the majority of the granitoids being geochemically similar to high-SiO_2 adakites (HSA). Their initial Nd ($\varepsilon_{Nd}=-12.5$ to -6.1) and Sr ($(^{87}Sr/^{86}Sr)_i=0.7054$–$0.7085$) isotopic compositions, however, distinguish them from adakites produced by partial melting of subducted slab and those produced by partial melting of the lower crust of the Yangtze Craton in the Late Mesozoic. The granitoid batholiths in the southeastern Hubei Province exhibit very low MgO ranging from 0.09 to 2.19 wt.% with an average of 0.96 wt.%, and large variations in negative to positive Eu anomalies (Eu/Eu*=0.22–1.4), especially the Tieshan granites and Yangxin granite porphyry (Eu/Eu*=0.22–0.73). Geochemical and Nd–Sr isotopic data demonstrate that these granitoids originated as partial melts of an enriched mantle source that experienced significant contamination of lower crust materials and fractional crystallization during magma ascent. Late Mesozoic granitoids in the southeastern Hubei Province of the Middle–Lower Yangtze River belt were dominantly emplaced in an extensional tectonic regime, in response to basaltic underplating, which was followed by lithospheric thinning during the early Cretaceous.

Keywords: Granitoid; Assimilation–fractional crystallization (AFC); Lithospheric extension; Middle–Lower Yangtze River belt

1. Introduction

The Middle–Lower Yangtze River belt (MLYRB) extends ~450 km from southeastern Hubei eastward to the Zhejiang Province over an area of ~30,000 km^2, and represents one of the most important economic mineral districts in China (Pan and Dong, 1999). The southeastern Hubei Province, in particular, represents an important region within this belt because it contains >50 Cu–Fe–Au–Mo–W deposits, including three large skarn Fe deposits (i.e. the Tieshan, Echeng and Jinshandian deposits) with Fe ore reserves of >100 million tonnes each and one large skarn Cu–(Fe) deposit (i.e. the Tonglushan deposit) with Cu ore reserves of 1.1 million tonnes and 5.7 million tonnes Fe) (Xie et al., 2006a). Although the Late Jurassic to Early Cretaceous period marks an important regional metallogenic event in the MLYRB (Xie et al., 2007), the

* Corresponding author. Institute of Mineral Resources, Chinese Academy of Geological Sciences, Beijing, 100037, China.
E-mail address: guiqingxie@sohu.com (G. Xie).

0024-4937/$ - see front matter © 2008 Elsevier B.V. All rights reserved.
doi:10.1016/j.lithos.2007.12.008

tectonic framework within which these deposits formed has not been well constrained. Late Mesozoic granitoids occur extensively throughout southeastern Hubei, and these are spatially and genetically associated with Fe–Cu skarn and Cu–Au–Mo–(W) porphyry–skarn deposits (e.g., Pan and Dong 1999; Mao et al., 2006; Xie et al., 2007). The tectonic framework that caused widespread Mesozoic magmatism in eastern China also has remained controversial (e.g. Li, 2000; Zhou et al., 2006). Based on geochemical evidence, most geologists consider the granitoids in the southeastern Hubei to have been derived from a mixed mantle–crust source, with assimilation–fractional crystallization controlling their composition (Mao et al., 1990; Shu et al., 1992; Zhou and Ren, 1994; Ma et al., 1994). In contrast, Wang et al. (2004) argued, on the basis of preliminary studies of quartz diorites from the Yinzu batholith, and a granodiorite porphyry in the Tongshankou stock in the southeastern Hubei (Fig. 1), that these intrusions have geochemical features similar to adakite which has been proposed originally as direct partial melt of subducted mid-ocean ridge basalt (Defant and Drummond, 1990), and concluded that they originated from partial melting of delaminated lower crust. To date, no systematic geochemical or Sr–Nd isotopic studies have been undertaken on these granitoids in the southeastern Hubei. In order to better constrain the origin of these granitoids, and thus better understand the genesis of the ore-forming events in the MLYRB, we present combined geochemical and Nd–Sr isotopic data for these rocks, and discuss their petrogenesis and tectonic setting.

2. Geological setting

The MLYRB is located on the northern margin of the Yangtze Craton and runs along the southeastern margin of the North China Craton and Dabieshan orogenic belt (insert of Fig. 1). It is bounded by the Xiangfan–Guangji fault (XGF) to the northwest, the Tangcheng–Lijiang regional strike–slip fault (TLF) to the northeast, and the Yangxing–Changzhou fault (YCF) to the south (insert of Fig. 1). The Precambrian basement rocks consist of metamorphic trondjhemite–tonalite–granodiorite gneisses and supracrustal rocks (felsic gneiss and muscovite quartz schist with intercalated amphibolite) which range in age from 2900 to 990 Ma (e.g. Chang et al., 1991; Zhai et al., 1992). This metamorphosed basement is uncomfortably overlain by a thick cover sequence consisting of Sinian clastic rocks, carbonate and chert, Cambrian chert nodules, mudstone and argillaceous limestone, Ordovician limestone and dolomitic limestone, Silurian clastic rocks, Devonian sandstone, Carboniferous sandstone, siltstone and limestone, Permian shale and limestone, and Triassic argillaceous clastic rocks (Chang et al., 1991; Zhai et al., 1992). In the MLYRB, Late Mesozoic magmatism mainly consists of Late Jurassic to Cretaceous calc–alkaline intrusive rocks and Early Cretaceous sub-alkaline to

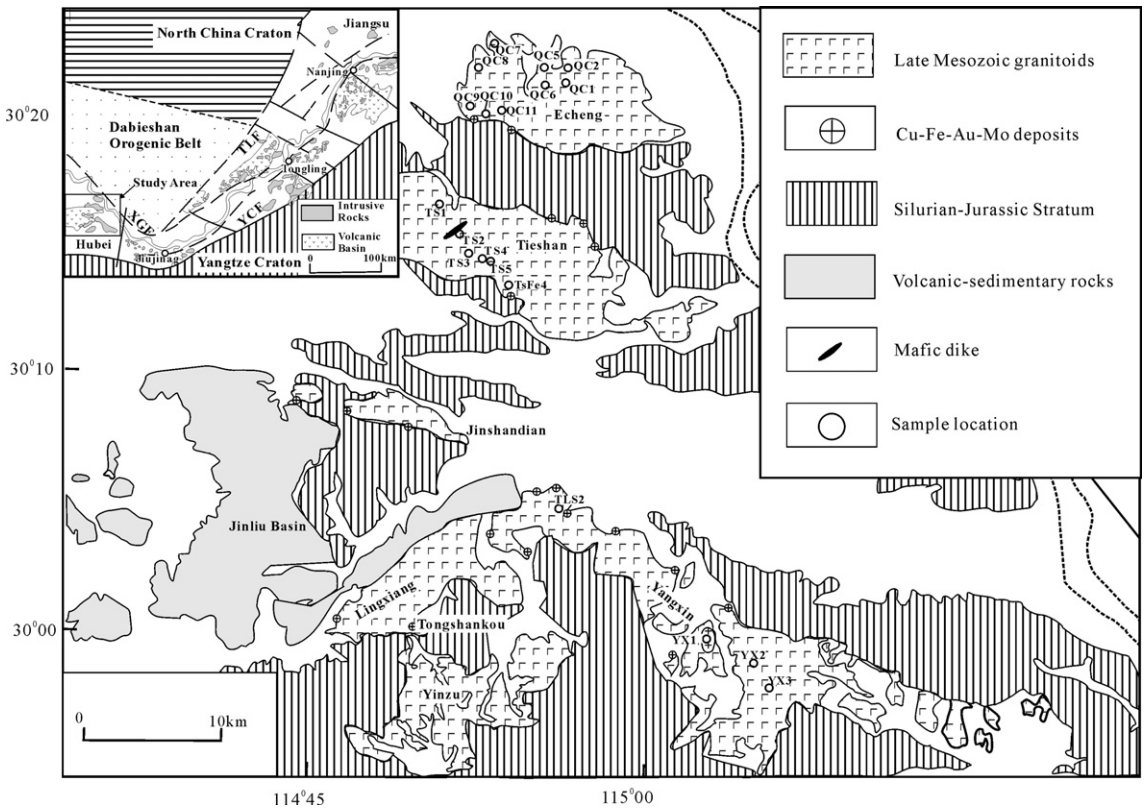

Fig. 1. Simplified geological map of the southeastern Hubei Province, showing the distribution of Late Mesozoic igneous rocks, Cu–Fe–Au–Mo deposits, and sample localities for this study (modified from Shu et al., 1992). Inset shows distribution of Late Mesozoic magmatic rocks in the MLYB, eastern China (modified from Mao et al., 1990), XGF: Xiangfan–Guangji Fault; TLF: Tangcheng–Lijiang Fault; YCF: Yangxing–Changzhou Fault.

alkaline volcanic rocks (Pei and Hong, 1995; Chen et al., 2001; Zhang et al., 2003; Xie et al., 2006b). In addition, minor Cretaceous quartz syenite, syenite, quartz monzonite, alkaline granite and phonolite are exposed in this region, and these have been classified as A-type granitoids (Mao et al., 1990).

Southeastern Hubei is situated in the western part of the MLYRB (Fig. 1). As shown in Fig. 1, Silurian to Middle Jurassic shallow-marine carbonate rocks, clastic rocks, and flysch sequences are widespread, with Late Mesozoic volcanic-sedimentary rocks restricted to in the western part of southeastern Hubei (Shu et al., 1992). Late Mesozoic granitic plutons and granodiorite porphyry stocks occupy approximately 17% of the area in the southeastern Hubei Province (Pan and Dong, 1999), including the: 1) Echeng granite, quartz diorite and monzonite (85 km^2 in outcrop); 2) Tieshan quartz diorite and monzonite (140 km^2); 3) Jinshandian quartz monzonite and diorite (16 km^2); 4) Lingxiang quartz diorite (54 km^2); 5) Yinzu granodiorite (54 km^2); and 6) Yangxin quartz diorite, monzonite and minor tonalite (215 km^2) (Fig. 1). In addition, several small granodiorite porphyry stocks are known to occur in this area (Shu et al., 1992). The ages of these granitoids are inadequately constrained by K–Ar and Rb–Sr isochron methods, giving ages that range from 205 Ma to 64 Ma (e.g. Zhou and Ren, 1994; Zhai et al., 1992; Pan and Dong, 1999). Zhou and Ren (1994) reported hornblende $^{40}Ar-^{39}Ar$ ages of 133.4±0.4 Ma and 135.9±0.5 Ma for the Tieshan quartz monzonite and Yangxin tonalite, respectively. Recent age determinations of quartz diorite in the Yangxin batholith and granite in Echeng batholith have yielded zircon SHRIMP U–Pb ages of 138.9±2.8 to 134±2 Ma (Ma et al., 2005; Xue et al., 2006) and 121.2±3.1 Ma (Xie G Q unpublished data), respectively. In the western part of southeastern Hubei, voluminous rhyolites and andesite, and minor basalts are present (Chang et al., 1991; Zhai et al., 1992). These have been dated by Xie et al. (2006b) at 128±2 Ma by the SHRIMP zircon U–Pb method.

3. Petrography

From this study, we have investigated three large granitoid intrusions, namely the Echeng, Tieshan and Yangxin batholiths. These felsic bodies typify the mode of occurrence, composition, and size of intrusive bodies in the region, and belong to the magnetite-series (Ishihara, 1977) or I-type granitoids (Pei and Hong, 1995). Brief petrological descriptions for each of the three batholiths are given below:

The Echeng granitoid in the northernmost part of the studied region is about 14 km long and 8 km wide, and has intruded a Late Triassic, intercalated sandstone–carbonate sequence. The granitoid consists predominantly of granitic, and subordinate quartz diorite and monzonite phases. The granites (sample QC 2, 5, 9, 10, 11) are characterized by moderate to coarse-grained texture, composed of K-feldspar (45–55%), plagioclase (13–18%), quartz (30–35%) and rare biotite, as well as accessory minerals such as zircon, titanite, magnetite and apatite. The quartz diorite (sample QC 7, 8) and monzonite (sample QC 1) predominantly consist of plagioclase (30–50%), K-feldspar (20–40%), quartz (10–15%) and hornblende (10–20%) and minor biotite (5%).

The geology and elemental geochemistry of the Tieshan intrusion have been well studied (e.g. Zhou and Ren, 1994; Ma et al., 1994), as the Fe deposits associated with this intrusion, such as the Daye deposit, represent important skarn deposits in China (Pan and Dong, 1999). The Tieshan granitoid intruded Late Triassic carbonate rocks, and has an exposed area of ~20 by 8 km. The intrusion is mainly composed of quartz diorite and subordinate monzonite, and minor gabbro at the southern margin, with rare gabbroic and dioritic enclaves and rare mafic dikes in the quartz diorite. The quartz diorites (sample TS 3, 4, 5) are predominantly composed of plagioclase (50–60%), K-feldspar (15–20%), quartz (5–15%), hornblende (7–15%) and rare biotite. Accessory minerals include zircon, titanite, magnetite and apatite. The monzonite (sample TS 1) and gabbro (sample TsFe 4) have mineral assemblages similar to the quartz diorite except the gabbro contains lesser quartz (2–7%) and more abundant mafic minerals. Mafic dikes (sample TS 2) intruded the Tieshan quartz diorite (Fig. 1), and these are medium-grained, mainly composed of plagioclase and biotite, with subordinate K-feldspar(kersantite; Rock et al., 1990).

The Yangxin intrusion is the largest batholith in the southeastern Hubei Province and outcrops over an area of 215 km^2. This intrusion consists dominantly of quartz diorite with minor granite porphyry that intruded Carboniferous to Late Triassic carbonate rocks. The quartz diorites (sample YX 2, 3, TLS 2) are fine to medium-grained, predominantly composed of plagioclase (50–60%), K-feldspar (8–15%), quartz (5–14%) and hornblende (10–15%) with minor biotite (~5%); accessory minerals include zircon, titanite, magnetite and apatite. Rare gabbroic and dioritic enclaves also occur in the quartz diorite. The granite porphyry (sample YX 1) is fine grained, mainly composed of plagioclase (55%), K-feldspar (20%), quartz (20%) with minor hornblende (3%) and biotite (2%).

4. Analytical methods

Major element analyses were carried out by a conventional wet chemical method at the Chemical Analytical Center, Institute of Geochemistry, Chinese Academy of Sciences (IGCAS). The analytical errors for major oxides are generally less than 2%. Trace elements and rare earth elements abundances were determined by solution ICP-MS performed at the ICP-MS Laboratory, also at IGCAS. The samples were digested by acid ($HF+HClO_4$) in bombs. Precision for most elements was typically better than 5% RSD, and the measured values for Zr, Hf, Nb and Ta were less than 10% in error compared to certified values. The detailed sample preparations, instrument operating conditions and calibration procedures follow those established by Qi and Grégoire (2000). The international standards GBPG-1 and the Chinese National standard GSR-1 were used for analytical quality control.

Samples for Sr and Nd isotopic analysis were dissolved in Teflon bombs with $HF+HNO_3$ acid on a hot plate for a week, and then separated by conventional cation-exchange techniques. The isotopic measurements were performed on a Finnigan MAT 262 multi-collector mass spectrometer at the Laboratory for Radiogenic Isotope Geochemistry, Institute of

Table 1
Major (%) and trace element (ppm) analyses for Late Mesozoic granitoids in the southeastern Hubei Province, MLYB, eastern China

Sample	QC1	QC2	QC5	QC6	QC7	QC8	QC9	QC10	QC11
Name of batholith	Echeng								
Rock type	QM	MG	MG	QD	QD	QD	CG	CG	CG
SiO_2	64.60	74.64	68.83	62.96	61.26	59.69	73.59	75.46	76.57
TiO_2	0.68	0.42	0.38	0.78	0.52	0.68	0.40	0.55	0.45
Al_2O_3	16.20	12.26	15.73	17.85	16.20	16.47	12.36	14.28	13.26
Fe_2O_3	0.30	0.30	0.75	0.91	2.61	2.09	0.91	0.20	0.10
FeO	0.13	0.12	0.10	0.28	1.36	1.90	0.10	0.05	0.07
MnO	0.05	0.06	0.04	0.03	0.08	0.07	0.01	0.03	0.05
MgO	1.08	0.22	0.40	1.65	1.97	2.19	0.56	0.43	0.09
CaO	4.87	1.51	1.58	3.90	5.55	5.59	1.76	0.73	0.68
Na_2O	5.04	5.57	4.29	5.92	3.78	3.79	2.86	3.36	5.19
K_2O	2.96	0.42	3.98	0.83	2.78	2.84	3.85	3.25	0.52
P_2O_5	0.62	0.29	0.29	1.11	0.47	0.49	0.28	0.22	0.18
LOI	3.32	3.55	3.98	3.22	2.74	3.66	2.82	0.87	2.39
Sum	99.85	99.36	100.35	99.44	99.32	99.46	99.50	99.43	99.55
K_2O /Na_2O	0.59	0.08	0.93	0.14	0.74	0.75	1.4	1.0	0.10
$Mg^{\#}$	0.85	0.54	0.52	0.76	0.53	0.55	0.57	0.80	0.55
Sc	7.04	5.52	2.92	13.4	10.5	11.0	2.94	3.57	5.11
V	73.9	22.8	13.6	158	136	141	16.0	5.65	5.58
Cr	18.5	5.16	87.8	21.4	20.2	24.3	2.93	5.67	16.7
Co	2.94	0.543	1.32	2.79	10.6	12.3	0.925	0.293	0.327
Ni	14.1	2.47	43.6	20.6	11.8	12.3	1.73	3.54	9.03
Rb	12.3	2.99	141	20.2	67.5	74.2	173	79.5	5.71
Sr	867	96.0	93.2	789	1290	1376	100	82	60
Y	16.9	12.9	22.1	29.3	15.5	15.1	23.2	5.17	6.50
Zr	69.9	212	71.1	309	108	71.5	214	163	130
Nb	13.0	14.7	20.9	24.2	7.67	8.90	24.4	31.4	24.4
Ba	210	45.0	367	121	1080	1227	388	189	26.3
La	44.2	56.4	46.4	116.5	39.3	50.3	28.6	5.83	3.67
Ce	76.5	90.2	78.1	174.2	73.6	89.7	56.5	15.4	14.0
Pr	7.90	8.82	7.92	18.0	8.79	10.2	7.13	1.42	1.14
Nd	29.5	31.1	27.1	64.5	38.4	42.1	24.4	5.48	4.54
Sm	3.97	3.93	4.90	8.23	6.22	6.68	3.93	0.930	1.05
Eu	1.38	0.856	0.556	3.36	1.98	1.83	0.623	0.133	0.073
Gd	4.31	3.10	4.01	7.58	4.78	4.94	3.90	0.900	0.936
Tb	0.458	0.395	0.666	1.06	0.559	0.630	0.604	0.149	0.166
Dy	3.15	1.93	3.33	4.95	2.65	3.06	3.60	0.93	1.22
Ho	0.538	0.460	0.748	0.946	0.524	0.478	0.722	0.197	0.221
Er	1.64	1.46	2.34	2.81	1.43	1.44	2.55	0.746	0.793
Tm	0.207	0.197	0.363	0.357	0.213	0.185	0.464	0.121	0.097
Yb	1.31	1.39	2.83	2.62	1.33	0.935	3.01	1.07	1.09
Lu	0.210	0.205	0.345	0.387	0.197	0.180	0.377	0.143	0.139
Hf	3.24	6.14	3.04	7.50	3.71	2.68	7.21	5.64	5.03
Ta	1.01	1.26	1.32	1.35	0.464	0.495	1.99	2.24	2.23
Pb	8.20	2.28	7.54	4.07	7.97	8.65	8.26	8.08	3.36
Th	10.2	14.1	27.4	7.99	9.25	11.3	18.4	17.1	25.5
U	2.00	2.26	2.82	5.66	1.09	1.48	2.31	2.39	1.98
Eu/Eu*	1.0	0.73	0.37	1.3	1.1	0.93	0.48	0.44	0.22

Sample	TS1	TS2	TS3	TS4	TS5	TsFe4	YX1	YX2	YX3	TLS2
Name of batholith	Tieshan						Yangxin			
Rock type	QD	L	QD	QD	QD	G	GP	QD	QD	QD
SiO_2	63.20	56.63	63.59	64.65	65.02	54.61	71.33	65.71	63.87	64.31
TiO_2	0.55	0.68	0.63	0.62	0.68	1.06	0.30	0.72	0.42	0.70
Al_2O_3	18.67	14.45	17.02	15.92	17.85	15.55	13.91	15.38	16.20	17.02
Fe_2O_3	2.01	3.93	2.05	1.23	1.40	2.79	0.82	2.00	0.48	2.61
FeO	0.92	2.78	0.72	0.70	1.00	1.70	0.25	0.59	0.10	0.43
MnO	0.08	0.10	0.07	0.07	0.06	0.13	0.05	0.11	0.08	0.10
MgO	1.20	4.84	1.34	0.62	1.07	3.36	0.60	1.23	0.96	0.71
CaO	4.42	5.98	3.84	4.96	3.56	9.97	1.40	4.38	4.87	6.40
Na_2O	3.83	3.05	3.81	3.57	3.83	3.78	2.89	3.60	5.39	3.33

(continued on next page)

Table 1 (*continued*)

Sample	TS1	TS2	TS3	TS4	TS5	TsFe4	YX1	YX2	YX3	TLS2
Name of batholith	Tieshan						Yangxin			
Rock type	QD	L	QD	QD	QD	G	GP	QD	QD	QD
K_2O	2.56	2.90	3.33	2.53	2.68	1.82	2.91	2.60	0.48	2.34
P_2O_5	0.37	0.52	0.40	0.39	0.33	0.67	0.23	0.34	0.40	0.33
LOI	1.77	3.54	2.70	4.39	2.33	3.54	4.81	3.11	6.06	1.48
Sum	99.58	99.40	99.50	99.65	99.81	98.98	99.50	99.77	99.31	99.76
K_2O /Na_2O	0.67	0.95	0.87	0.71	0.70	0.48	1.01	0.72	0.09	0.70
$Mg^{\#}$	0.48	0.62	0.53	0.42	0.50	0.63	0.57	0.52	0.79	0.35
Sc	8.01	19.58	5.87	4.74	6.35	12.9	2.86	6.18	8.89	6.91
V	56.3	135	58.3	38.8	38.6	128	26.7	73.3	75.5	47.3
Cr	25.8	216	16.2	33.0	30.0	44.7	6.93	16.5	23.2	12.5
Co	7.56	19.3	4.79	5.28	4.10	17.4	2.85	9.35	5.26	7.40
Ni	16.4	52.5	11.9	20.4	17.1	34.0	4.34	7.89	10.5	9.43
Rb	62.9	91.8	54.4	68.0	73.3	49.4	166	156	29.0	87.5
Sr	1431	765	1269	1025	1220	2405	329	798	456	969
Y	15.4	17.8	12.9	11.2	15.0	15.4	5.25	13.4	12.6	14.5
Zr	161	141	39.4	164	205	64.6	130	131	158	150
Nb	12.5	10.6	8.16	8.49	11.7	5.67	6.44	16.3	15.7	13.7
Ba	1192	1216	1466	1048	1158	1367	939	785	43.7	917
La	51.5	54.4	53.5	38.9	46.8	69.0	25.7	48.9	39.6	44.5
Ce	100.8	103.8	101.0	76.1	89.3	145.3	41.4	83.9	75.8	87.4
Pr	11.3	11.8	11.1	8.61	10.6	17.6	4.55	8.63	8.07	9.75
Nd	39.4	40.3	37.5	31.7	35.0	61.4	16.1	30.5	28.6	30.6
Sm	6.57	7.59	5.09	5.30	5.83	10.1	2.10	4.84	4.59	4.84
Eu	1.71	1.86	1.37	1.25	1.20	2.50	0.839	1.56	1.04	1.42
Gd	5.16	5.71	4.54	3.91	4.98	8.29	1.59	4.47	3.85	3.94
Tb	0.601	0.616	0.521	0.410	0.679	0.793	0.183	0.570	0.446	0.536
Dy	3.30	3.74	2.98	2.64	2.81	3.64	0.926	2.07	2.02	3.22
Ho	0.583	0.814	0.484	0.409	0.592	0.631	0.143	0.400	0.448	0.544
Er	1.68	1.97	1.45	1.23	1.50	1.40	0.468	1.22	1.22	1.24
Tm	0.224	0.298	0.182	0.150	0.269	0.204	0.054	0.146	0.155	0.185
Yb	1.32	1.57	0.947	0.929	1.00	1.10	0.340	1.20	1.25	1.25
Lu	0.209	0.278	0.159	0.143	0.222	0.162	0.042	0.225	0.172	0.285
Hf	3.29	2.75	1.08	3.32	4.54	1.63	4.42	5.23	5.50	3.55
Ta	0.681	0.654	0.559	0.642	0.648	0.288	0.478	1.46	1.11	0.909
Pb	9.54	7.57	9.57	10.7	16.6	11.6	19.3	8.39	3.99	13.0
Th	8.85	14.9	10.3	7.24	10.0	5.06	7.51	15.5	16.1	12.1
U	1.52	3.42	1.80	1.53	1.78	1.26	1.66	4.54	5.24	2.65
Eu/Eu*	0.87	0.83	0.85	0.80	0.67	0.81	1.4	1.0	0.74	0.97

Note: QM = quartz monzonite, MG = moderate-grained granite, CG = coarse-grained granite, QD = quartz diorite, L = lamprophyre, G = gabbro, GP = granite porphyry.

Geology and Geophysics (Beijing), Chinese Academy of Sciences. Measured Sr and Nd isotopic ratios were normalized using an $^{86}Sr/^{88}Sr$ value of 0.1194 and a $^{146}Nd/^{144}Nd$ value of 0.7219, respectively. $^{87}Rb/^{86}Sr$ and $^{147}Sm/^{144}Nd$ ratios were calculated using the Rb, Sr, Sm and Nd abundances measured by ICP-MS. Analyses of standards during the period of analysis are as follows: NBS987 $^{87}Sr/^{86}Sr = 0.710254 \pm 11 (2\sigma)$ ($n = 27$); Ames Nd standard $^{143}Nd/^{144}Nd = 0.512145 \pm 12$ (2σ) ($n = 15$). Major and trace element composition and Nd–Sr isotopic data for granitoids in the Southeastern Hubei are listed in Tables 1 and 2, respectively.

5. Results

5.1. Major and trace elements

As shown in a classification diagram using $K_2O + Na_2O$ versus SiO_2 (Fig. 3; Middlemost, 1994), the Tieshan intrusion is dominated by quartz diorite, quartz monzonite and diorite, the Yangxin intrusion by quartz diorite and quartz monzonite, and the Echeng intrusion by granite, quartz diorite and quartz monzonite. The total alkali versus silica classification of Irvine and Baragar (1971) shows that most samples belong to the sub-alkaline series, with some samples falling into the alkaline series (Fig. 2). In general, the samples have high alkali with $K_2O + Na_2O$ ranging from 5.60 to 8.00% and high K_2O contents from 0.42 to 3.98% (most are between 1.82 and 3.98%), and fall into the high-K and middle-K calc-alkaline field in a SiO_2 versus K_2O diagram (Fig. 3), except for samples from the Echeng granite and Yangxin granite porphyry (Table 1). The Tieshan and Yangxin batholiths are characterized by large variations in chemical composition and show similar variation trends in Harker plots (Fig. 4), but with the former ($SiO_2 = 54.61$–65.02%, $MgO = 0.62$–4.84%) being slightly less differentiated than the latter ($SiO_2 = 64.31$–71.33%, $MgO = 0.60$–1.23%). The Echeng batholith also exhibits similar trend for the major oxides when compared

Table 2
Sr and Nd isotopic compositions of Late Mesozoic granitoids

Sample no.	Sm	Nd	$^{147}Sm/^{144}Nd$	$^{143}Nd/^{144}Nd$	2δ	$(^{143}Nd/^{144}Nd)_i$	$\varepsilon_{Nd}(t)$
TS1	6.57	39.4	0.1008	0.512104	0.000013	0.5120	−8.8
TS2	7.59	40.3	0.1139	0.512175	0.000013	0.5121	−7.6
TS3	5.09	37.5	0.0821	0.512024	0.000012	0.5120	−10.0
TS5	5.83	35.0	0.1007	0.512127	0.000015	0.5120	−8.3
TsFe4	10.13	61.4	0.0998	0.512147	0.000015	0.5121	−7.9
YX1	2.10	16.1	0.0788	0.512095	0.000013	0.5120	−8.5
YX2	4.84	30.5	0.0960	0.512233	0.000014	0.5121	−6.1
YX3	4.59	28.6	0.0971	0.512218	0.000014	0.5121	−6.4
TLS2	4.84	30.6	0.0958	0.512204	0.000013	0.5121	−6.7
QC1	3.97	29.5	0.0815	0.511973	0.000012	0.5119	−11.2
QC2	3.93	31.1	0.0764	0.511903	0.000012	0.5118	−12.5
QC5	4.90	27.1	0.1093	0.511996	0.000013	0.5119	−11.2
QC6	8.23	64.5	0.0772	0.512057	0.000012	0.5120	−9.5
QC7	6.22	38.4	0.0981	0.512136	0.000012	0.5121	−8.3
QC9	3.93	24.4	0.0975	0.511986	0.000012	0.5119	−11.2
QC10	5.12	21.7	0.1026	0.511998	0.000013	0.5119	−11.0

Sample no.	Rb	Sr	$^{87}Rb/^{86}Sr$	$^{87}Sr/^{86}Sr$	2δ	$(^{87}Sr/^{86}Sr)_i$	$\varepsilon_{Sr}(T)$
TS1	62.9	1431	0.1272	0.707404	0.000013	0.7072	4.0
TS2	91.8	765	0.3475	0.706095	0.000011	0.7054	1.5
TS3	54.4	1269	0.1241	0.707362	0.000011	0.7071	3.9
TS5	73.3	1220	0.1737	0.707497	0.000010	0.7072	4.0
TsFe4	49.4	2405	0.0594	0.706890	0.000012	0.7068	3.4
YX1	165.5	329	1.4576	0.708646	0.000011	0.7058	2.0
YX2	156.4	798	0.5667	0.706785	0.000013	0.7057	1.8
YX3	29.0	456	0.1838	0.707280	0.000013	0.7069	3.6
TLS2	87.5	969	0.2615	0.706501	0.000012	0.7060	2.3
QC1	12.3	867	0.0409	0.707868	0.000011	0.7078	4.8
QC2	2.99	96.0	0.0900	0.708660	0.000014	0.7085	5.8
QC5	141.3	93.2	4.3881	0.715314	0.000014	0.7078	4.8
QC6	20.2	789	0.0741	0.708555	0.000012	0.7084	5.7
QC7	67.5	1290	0.1515	0.706746	0.000014	0.7065	3.0
QC9	172.7	100	4.9772	0.715285	0.000011	0.7067	3.3
QC10	79.5	81.8	2.8110	0.712644	0.000013	0.7078	4.9

Sample Numbers and locations are the same as in Table 1. Note: $(^{87}Sr/^{87}Sr)^0_{UR}=0.7045$, $(^{87}Rb/^{86}Sr)^0_{UR}=0.0827$, $(^{143}Sm/^{144}Nd)^0_{CHUR}=0.51238$, $(^{143}Nd/^{144}Nd)^0_{CHUR}=0.1967$; $\lambda_{Rb}=1.42\times10^{-11}$/year, $\lambda_{Sm}=6.5\times10^{-12}$/year (Rollinson, 1993).

to the samples from the Tieshan and Yangxin intrusions. In particular, the quartz diorite and monzonite show similar chemical compositions, and are significantly less differentiated than granite with SiO_2 ranging between 68.83 and 76.57% and MgO between 0.22 and 0.56% (Table 1, Fig. 4). As shown in Fig. 4, these batholiths are characterized by obvious negative correlations between SiO_2 and MgO, CaO, TiO_2, FeOt, Al_2O_3, P_2O_5, MnO, indicating the effects of fractional crystallization during magmatic evolution.

All granitoids in the Southeastern Hubei are characterized by a general LREE (light rare earth elements)-enrichment ($La_N/Yb_N=2.3–50.9$) and variable bulk REE (rare earth elements) concentrations (29.1–405 ppm) (Fig. 5, Table 1), with positive to negative Eu anomalies ($Eu/Eu^*=0.22–1.3$). In particular, the Echeng granites and Yangxin granite porphyry display strong negative Eu anomalies ($Eu/Eu^*=0.22–0.73$). As shown in Fig. 5c, the gabbroic and dioritic mafic enclaves ($SiO_2<55\%$) have REE patterns similar to those of the Tieshan quartz diorite and lamprophyre (Ma et al., 1994).

On primitive mantle-normalized variation diagrams (Fig. 6), the Tieshan and Yangxin batholiths display generally similar profiles that are characterized by enrichment in LREE and Rb, Th, U, Pb, and significant depletion in Nb and Ta (Fig. 6c, d). The Echeng quartz diorite and monzonite show enrichment in Th, Pb, Sr and LREE, and significant depletion in Nb and Ta (Fig. 6b), similar to the Tieshan and Yangxin granitoids. In contrast, the Echeng granites are enriched in Th and Pb and depleted in Ba and Sr, without depletion in Nb and Ta (Fig. 6a). From Fig. 6c, the gabbroic and dioritic enclaves ($SiO_2<55\%$) show similar trace element characteristics to quartz diorite and lamprophyre from the Tieshan batholith (Ma et al., 1994).

5.2. Nd–Sr isotopes

Nd and Sr isotopic data have been obtained from representative samples of the Tieshan, Yangxin and Echeng batholiths (Table 2). The Tieshan batholith show elevated initial ε_{Nd} values ranging from −10.0 to −7.6, and moderate $(^{87}Sr/^{86}Sr)_i$ ratios from 0.7054 to 0.7072 .These values are comparable with those of the Yangxin quartz diorite and granitic porphyry that have ε_{Nd} values ranging from −8.5 to −6.1, and $(^{87}Sr/^{86}Sr)_i=0.7057–0.7069$. The Echeng granitoids have slightly lower initial ε_{Nd} (−12.5 to −8.3) but slightly higher $(^{87}Sr/^{86}Sr)_i$ (0.7065 to 0.7085) (Fig. 7).

6. Discussion

6.1. Petrogenesis

As shown in Table 1, the Tieshan, Yangxin and Echeng batholiths are characterized by intermediate to high concentrations of SiO_2 (54.61–76.57 wt.%) Na_2O (2.89–5.57 wt.%), and Sr (60.5–1220 ppm), but low Y (5.17–29.3 ppm) and Yb (0.34–2.83 ppm), and have geochemical features similar to high-silica adakite (HAS) (see reviews in Martin et al., 2005) (Figs. 4a, 8), as they fall into the adakite field on Sr/Y versus Y, and $(La/Yb)_N$ versus Yb_N diagrams (Fig. 9) except for the samples from the Echeng granite and Yangxin granite porphyry. Over the past decade, attention has been drawn to the origin of adakites (see reviews in Castillo, 2006) , with proposed models including: (1) melting of subducted oceanic slab (e.g. Defant and Drummond, 1990), (2) melting of delaminated lower crust (Xu et al., 2002; Wang et al., 2004; 2006) or underplated basaltic crust (e.g. Atherton and Petford, 1993), (3) assimilation and fractional crystallization (AFC) processes involving basaltic magmas (Castillo et al., 1999; Macpherson et al., 2006) and (4) melting of mantle peridotite previously metasomatized by slab-melts (e.g. Jiang et al. 2006).

It is generally accepted that the MLYRB comprises one of the most important Late Mesozoic igneous rock provinces in eastern China (e.g. Xie et al., 2005a). However, whether Late Mesozoic magmatism in eastern China was related to westward subduction of the paleo-Pacific Plate remains controversial (e.g. Li, 2000; Zhou et al., 2006). As shown in Fig. 7a, the low ε_{Nd} (−12.5 to −6.1) and moderate $(^{87}Sr/^{86}Sr)_i$ (0.7054 to 0.7084) of the Tieshan, Yangxin and Echeng granitoids are distinct from those of mid-oceanic-ridge basalt (MORB) (Defant and Drummond, 1990), indicating that these granitoids could not have been directly derived from partial melting of the subducted slab.

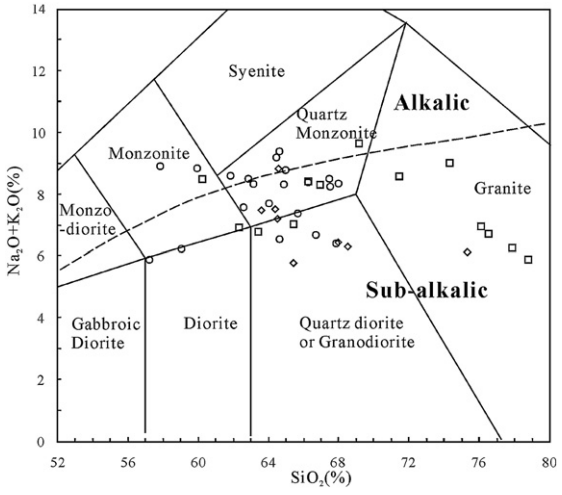

Fig. 2. Total alkalis (K_2O+Na_2O) versus SiO_2 diagram for Late Mesozoic granitoids (compositional fields from Middlemost, 1994), the division between alkaline and sub-alkaline is after Irvine and Baragar (1971). □: Echeng batholith (this study; Zhou and Ren, 1994), ◇: Yangxin batholith (this study; Zhou and Ren, 1994) , ○: Tieshan batholith (this study; Ma et al., 1994; Zhou and Ren, 1994).

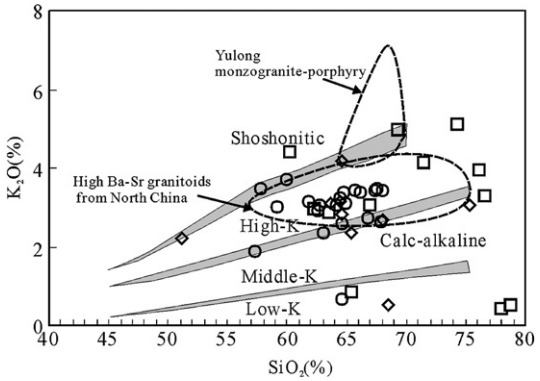

Fig. 3. K_2O versus SiO_2 diagram for Late Mesozoic granitoids (compositional fields from Rollinson, 1993). For comparison, enriched mantle-derived Yulong monzogranite-porphyry (Jiang et al., 2006) and high Ba–Sr granitoids from North China (Qian et al., 2003) are also shown. Symbols and references are the same as in Fig. 2.

More recently, some Late Mesozoic granitoids with an adakitic affinity have been recognized in eastern China and these are referred to as 'Chinese C-type' adakite (hereafter referred to as C-adakite) (Zhang et al., 2001), the origin of these adakitic rocks is poorly understood. Some Cretaceous granitic rocks in the Tongling and Nanjing (insert of Fig. 1) show affinities with C-adakite and have been proposed to originate from partial melting of delaminated lower crust and interaction with mantle rocks (Xu et al., 2002; Wang et al., 2006). However, several lines of evidence strongly suggest that the Tieshan, Yangxin and Echeng batholiths could not have directly originated from partial melting of basaltic lower crust:

(1) These granitoids span a wide range of K_2O/Na_2O from 0.08 to 1.4 with an average of 0.66, and are thus significantly different from delaminated lower crust-derived C-adakite that are characterized by enrichment in potassium and K_2O/Na_2O ratios of around unity (Xiao and Clemens, 2007). Moreover, experimental studies have demonstrated that adakitic magmas derived directly from lower crustal mafic rocks usually show high Na_2O (>4.3 wt.%) rather than high K_2O (Rapp and Watson, 1995). Although they exhibit high Na_2O (Figs. 3, 4h, 8), the granitoids investigated in this study also have elevated K_2O, Ba and Sr contents, similar to high Ba–Sr granitoids from, for example, the North China Craton and the Yulong granite porphyry, all of which derived directly from an enriched mantle source (Qian et al., 2003; Jiang et al., 2006).

(2) Interaction between adakitic melt from delaminated lower crust and the mantle can increase the mantle fingerprint, and give rise to elevated MgO, Cr, and Ni concentrations, as demonstrated by the Xinglonggou adakites in the North China Craton which have unusually high MgO (on average 3.7%, but up to 5.7%), Cr (127–402 ppm), and Ni (82–311 ppm) concentrations (Gao et al. 2004). Adakites derived from a peridotitic mantle wedge modified by reaction with felsic slab-melts are characterized by low SiO_2 contents and elevated MgO, Cr, Ni, V

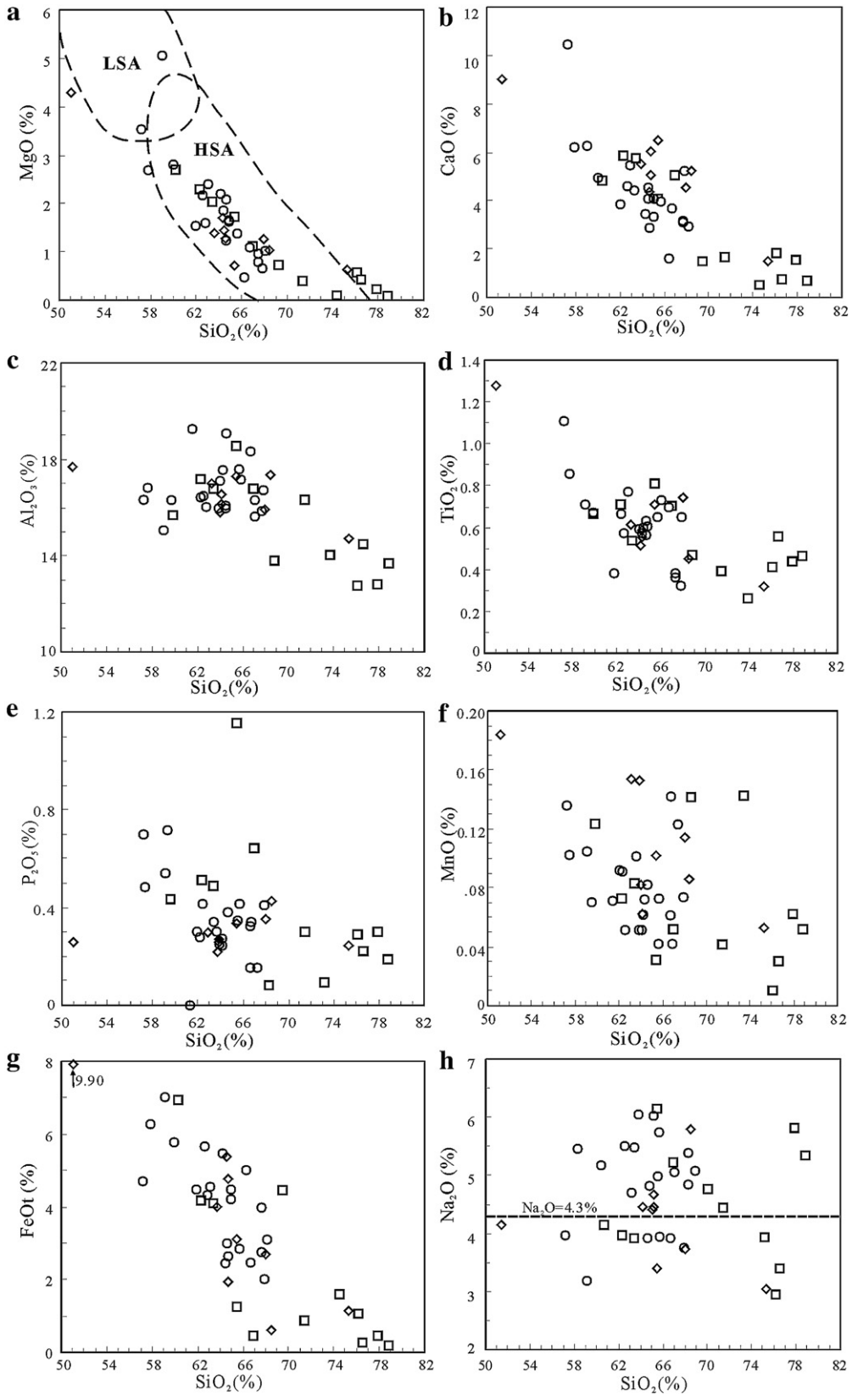

Fig. 4. Major elements variation diagrams for Late Mesozoic granitoids. LSA (low-SiO_2 adakites) and HSA (high-SiO_2 adakites) are after Martin et al., 2005. Symbols and references are the same as in Fig. 2.

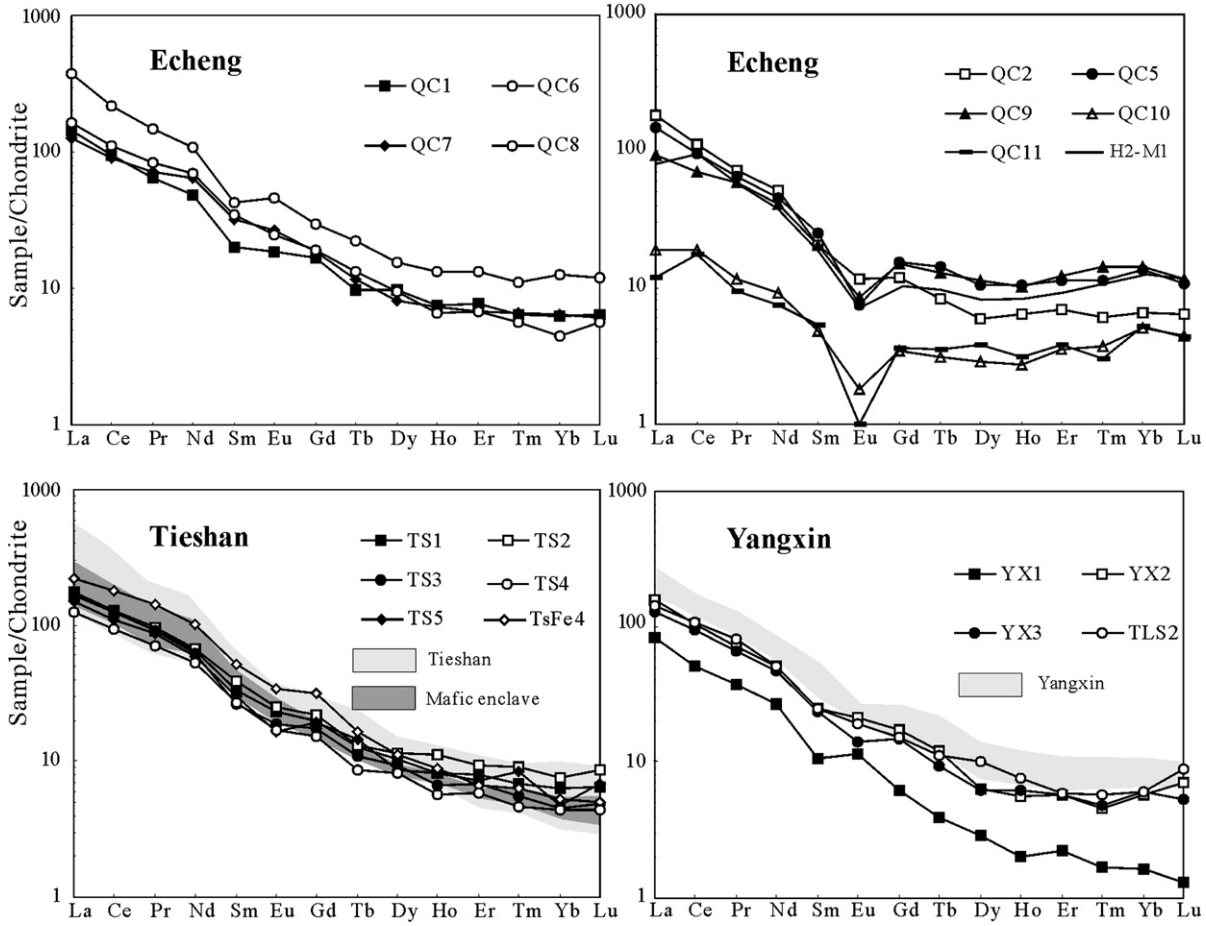

Fig. 5. Chondrite-normalized REE patterns for Late Mesozoic granitoids. Normalization values are after Boynton, 1984. Sample H2-M1 is after Zhou and Ren, 1994. The shaded area and mafic enclave of Tieshan are after Zhou and Ren, 1994; Ma et al., 1994, respectively. The shaded area for Yangxin is after Zhou and Ren, 1994.

contents (e.g. Martin et al., 2005). However, except for the lamprophyre (TS2) and gabbro (TSFe4) samples from the Tieshan intrusion, these granitoids from the southeastern Hubei Province exhibit very low MgO ranging from 0.09 to 2.19% with an average of 0.96%, and low Cr (2.93–87.8 ppm) and Ni (2.47–52.5 ppm) concentrations, respectively.

(3) Fig. 7 shows that the Nd and Sr isotopic ratios of granitoids in the southeastern Hubei ($\varepsilon_{Nd}=-12.5$ to -6.1, $(^{87}Sr/^{86}Sr)_i=0.7054$ to 0.7085) are different from those of lower crust ($\varepsilon_{Nd}=-33$ to -20, $(^{87}Sr/^{86}Sr)_i=07010$–$0.712$) in the Yangtze Craton (Jahn et al., 1999). Furthermore, geochemical data suggest that the lower crust in eastern China as a whole is characterized by about 57 wt.% SiO_2, which is in contrast to generally accepted models of the composition of mafic lower crust (Gao et al., 1998).

As shown in Fig. 7b, Nd–Sr compositions of the Tieshan, Yangxin and Echeng batholiths, especially the Yangxin quartz diorite, and Tieshan quartz diorite, are comparable with those of Late Mesozoic basalt and mafic intrusions elsewhere in the MLYRB (Chen et al., 2001; Wang et al., 2004, 2006; Yan et al., 2005; Xie et al., 2005b), suggesting considerable input from a mantle component to these granitoids. The quartz diorites from Echeng, Yangxin and Tieshan have lower SiO_2 and $(^{87}Sr/^{86}Sr)_i$, but higher K_2O, ε_{Nd}, Ba and Sr than the Echeng granite(Figs. 3, 7 and 8), indicating that the former show affinities with a more metasomatised lithospheric mantle than the latter (e.g. Qian et al., 2003; Jiang et al., 2006). Except for Echeng granite, the quartz diorites from Echeng, Yangxin and Tieshan are geochemically comparable to the mafic enclaves with respect to its trace element and REE patterns, indicating the involvement of an enriched metasomatised lithospheric mantle source in formation of these granitoids (Ma et al., 1994).The Mesozoic granitoids of the MLYRB are I-type granites with low while rock$\delta^{18}O$ (8–10‰) of whole-rock, further implying that the parental magma was a mixture of mantle-derived and crustal material that formed by partial melting of metamorphosed basement (Pei and Hong, 1995). Finally, recent studies have demonstrated that skarn Cu–Fe–Au–Mo deposits such as the Tonglushan Cu–Fe deposit, which are genetically associated with the Yangxi batholith, exhibit high Re contents in molybdenite ranging from 175.7 to 665.4 ppm (Xie et al., 2007), implying evolution of a mantle-derived fluid as part of the metallogenic system (Stein et al., 2001). Thus, in summary, the combined data point to the likely derivation of the parental magma from an enriched lithospheric mantle to generate the Mesozoic granitoids in the southeastern Hubei.

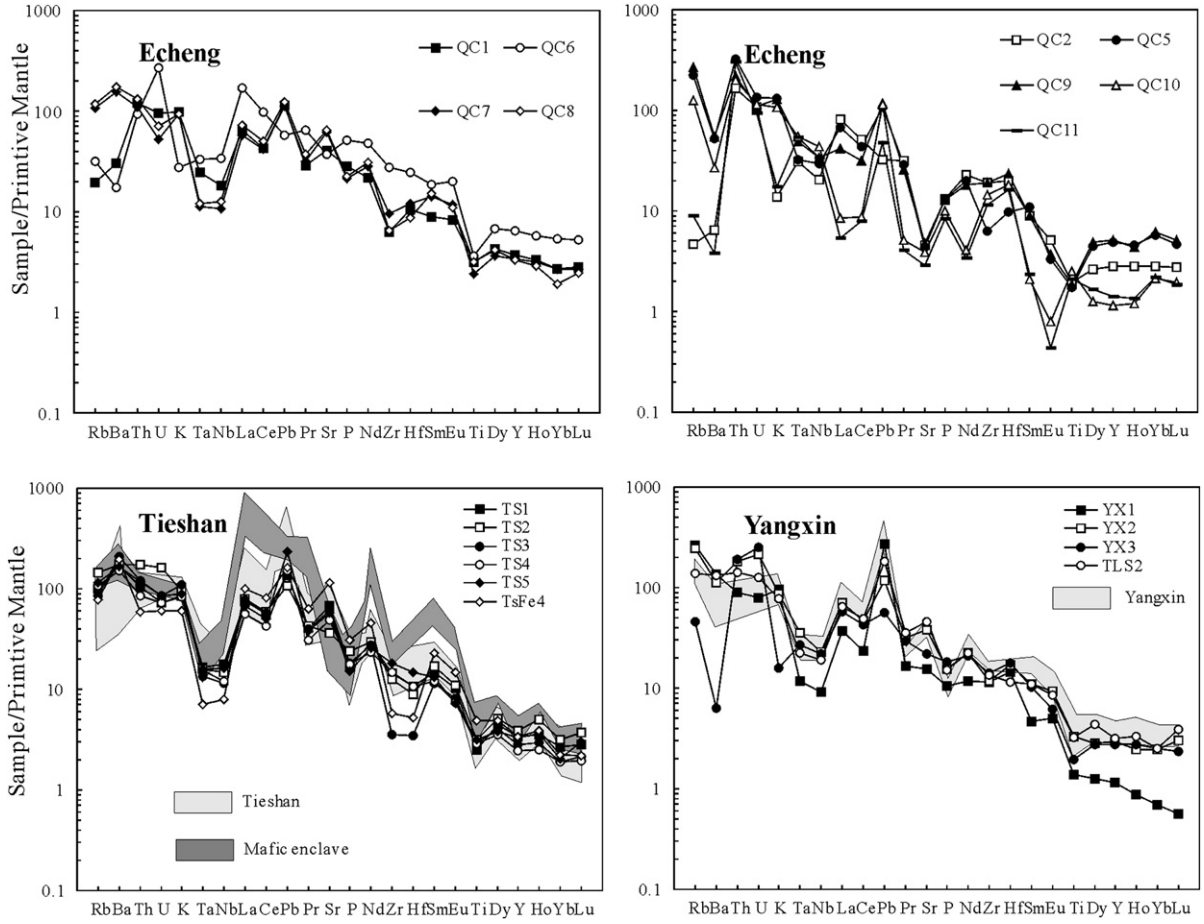

Fig. 6. MORB-normalized incompatible element spiderdiagrams for Late Mesozoic granitoids. Normalization values after Sun and McDonough, 1989. Symbols and references are the same as in Fig. 5.

The relatively low MgO concentration of the Tieshan, Yangxin and Echeng batholiths (Table 1) suggests that significant degrees of fractional crystallization of ferromagnesian phases such as hornblende and pyroxene occurred during the formation of these granitoids. This notion is supported by the decreasing trends in MgO, CaO, Al_2O_3 and TiO_2 with increasing SiO_2 (Fig. 4). In general, feldspar is the most important fractionating phase during granitic evolution, and the size of the negative Eu anomaly can be used as a measure of the degree of this feldspar fractionation (Rollinson, 1993). Strongly negative Eu depletion (Eu/Eu* 0.22–0.72) in the Echeng granite is probably the result of feldspar fractionation, as also suggested by the moderate negative correlation between Eu/Eu* versus Th and SiO_2 (Fig. 10). The above evidence suggests that magmas responsible for Late Mesozoic granitoids in the southeastern Hubei were derived from an enriched lithospheric mantle source, and were subsequently modified by assimilation–fractional crystallization (AFC) processes during their ascent, This process is also indicated by in the $(^{87}Sr/^{86}Sr)_i$ and $\varepsilon_{Nd}(t)$ versus SiO_2 plot (DePaolo, 1981) (Fig. 11). Geochemical modeling shows that these granitoids were produced by AFC process in which 5–30% lower crust was involved in the magma generation (Fig. 7b). As shown in Figs.4 a and 8, these granitoids are geochemically similar to high-SiO_2 adakite(HSA) which is considered to represent subducted basaltic slab-melts that have reacted with peridotite during ascent through the mantle wedge (Martin et al., 2005). The scenario proposed here for the generation and petrogenesis of Mesozoic granitoids in the MLYRB is similar to the formation of Cenozoic adakitic rocks in Camiguin Island, Philippines, which were derived from a slab fluid-metasomatized mantle wedge and experienced AFC processes prior to eruption (Castillo et al., 1999).

6.2. Tectonic setting

From the Jurassic to Cretaceous, the MLYRB experienced a phase of extensive magmatism that developed throughout eastern China (Zhou et al., 2006). Among the igneous rocks produced, intermediate-acid intrusive rocks are dominant, followed by widespread deposition of Cretaceous volcanic rocks (Mao et al., 1990). Based on published age information and the data presented in this study, we suggest that the widespread Late Mesozoic granitic magmatism in the southeastern Hubei occurred in an extensional setting, as substantiated by the following three lines of evidence:

(1) The data presented above show that the emplacement of these granitoids took place between 136 and 121 Ma, coeval with the emplacement of early Cretaceous A-type granites elsewhere in the MLYRB based on, for example,

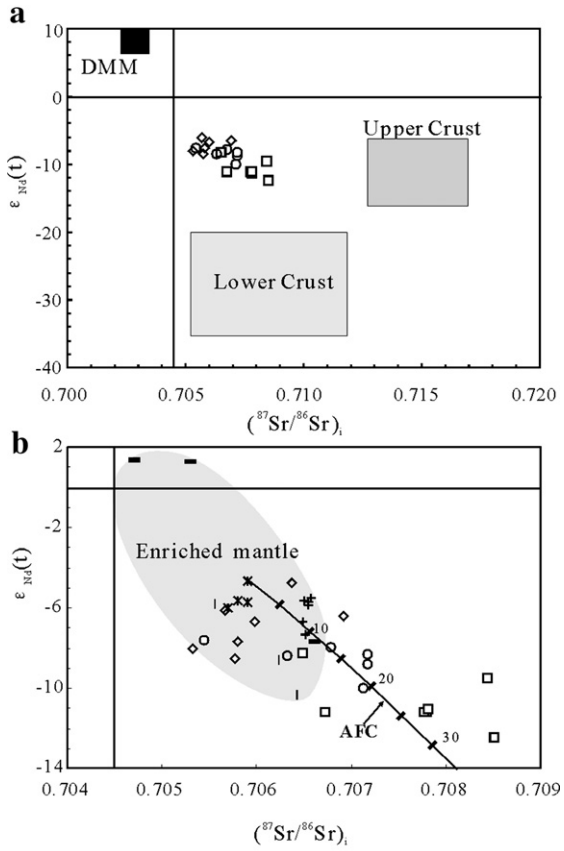

Fig. 7. Nd and Sr isotopic variation diagram for Late Mesozoic granitoids. For comparison, Late Mesozoic basalt and mafic intrusions in the MLYB are also shown. DMM, Lower crust and upper crust taken from Jahn et al. (1999): Gushan monzogabro (125 Ma) (Chen et al., 2001). *: Basic shoshonitic rocks (SiO_2<55%) (140–125 Ma) (Wang et al., 2006).+: Basalt (115 Ma) (Yan et al., 2005). Other symbols and references are the same as for Fig. 2. The modeling process for the open system AFC for Late Mesozoic granitoids in southeastern Hubei followed by DePaolo (1981), and the numbers in Fig. 7b indicate the percentages of participation of the lower crust materials, and the bulk coefficient for Sr (K_DSr) and Nd (K_DNd) are 0.5 and 0.8, respectively, r=0.75, and the calculated parameters of Sr, $(^{87}Sr/^{86}Sr)_i$, Nd and $\varepsilon_{Nd}(t)$ are 320 ppm, 0.7120, 20 ppm and −28 for lower crust after Jahn et al. (1999), and the least evolved shoshonitic rocks 98LZ060 (Sr=899 ppm, $(^{87}Sr/^{86}Sr)_i$=0.7059, Nd=59.22 ppm, $\varepsilon_{Nd}(t)$=−4.66) in the western Tongling (insert of Fig. 1) is assumed as the composition of enriched lithosphere mantle beneath the MYLB as proposed by Wang et al., 2006. AFC: Assimilation–fractional crystallization.

SHRIMP U–Pb zircon ages of 125±2 Ma for the Huashan riebeckite granite, a whole-rock Rb–Sr isochron age of 133.1±2.5 Ma for the Huangmeijian quartz syenite, and a SHRIMP zircon age of 136±3 Ma for the adakitic shaxi quartz diorite porphyries (e.g. Wang et al., 2006 and references therein), all of which have been interpreted to have formed in an extensional continental setting in the MLYRB.

(2) Recent SHRIMP U–Pb zircon dating has indicated that volcanic rocks from the Niuwu and Jinliu Basins in the MLYRB were also deposited between 131 and 127 Ma (Zhang et al., 2003; Xie et al., 2006b). Volcanic rocks from the Jinliu, Zhenjiang, Fanchang and Huaining basins, and which are synchronous with the emplacement of the A-type granitoids in the MLYRB, are characterized by bimodal characteristics (Xie et al., 2006b; Xie G Q unpublished data).

(3) Widespread Late Mesozoic mafic dikes are commonly spatially associated with these granitoids in the MLYRB (see Fig. 2).Although most of the dikes have not been precisely dated, based on geological evidence, the mafic dikes were dominantly emplaced during the late Jurassic to early Cretaceous in eastern China (Xie et al., 2005b, 2006c). An exception is a spessartite from the Wushan skarn copper ore districts nearby Jiujiang(Fig. 1) that has been dated at 143.5–139.7 Ma by the whole-rock K–Ar method (Xie et al., 2005b).

A-type granites, bimodal volcanic rocks and mafic dikes commonly occur either in post-orogenic or anorogenic settings (e.g. Hall, 1982; Whalen et al., 1987), we therefore propose that the Late Mesozoic granitoids in the southeastern Hubei were emplaced into an extensional setting. Although adakitic magmatism is usually associated with convergent plate setting (see Gutscher et al., 2000, for a review), at least some adakitic rocks can be shown to have formed unambiguously in an extensional tectonic regime (e.g. Wang et al., 2006).

Studies of mantle xenoliths in the North China Craton (Menzies et al., 1993) and Yangtze Craton (Xu et al., 2000) have indicated that ancient continental lithosphere has been removed and replaced by thinner and more fertile mantle material during

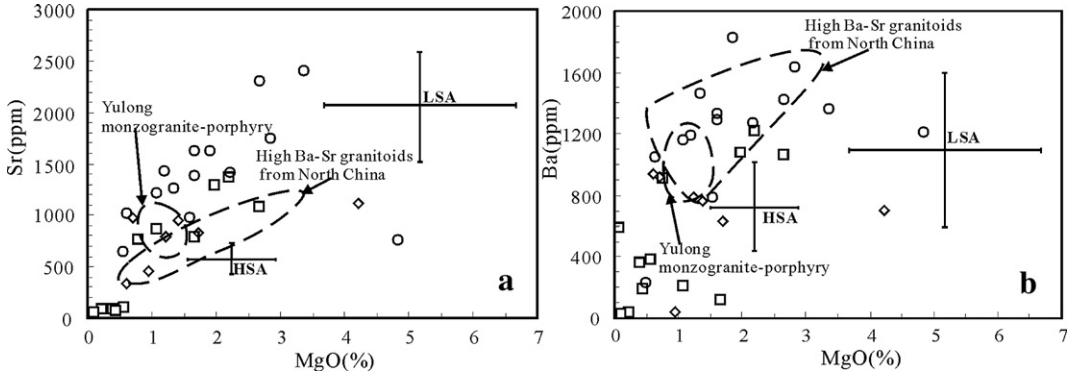

Fig. 8. MgO versus Sr (a) and Ba (b) diagrams for Late Mesozoic granitoids. For comparison, enriched mantle-derived Yulong monzogranite-porphyry (Jiang et al., 2006) and high Ba–Sr granitoids from North China (Qian et al., 2003) are also shown. LSA (low-SiO_2 adakites) and HSA (high-SiO_2 adakites) are after Martin et al. (2005). Symbol and reference are the same as in Fig. 2.

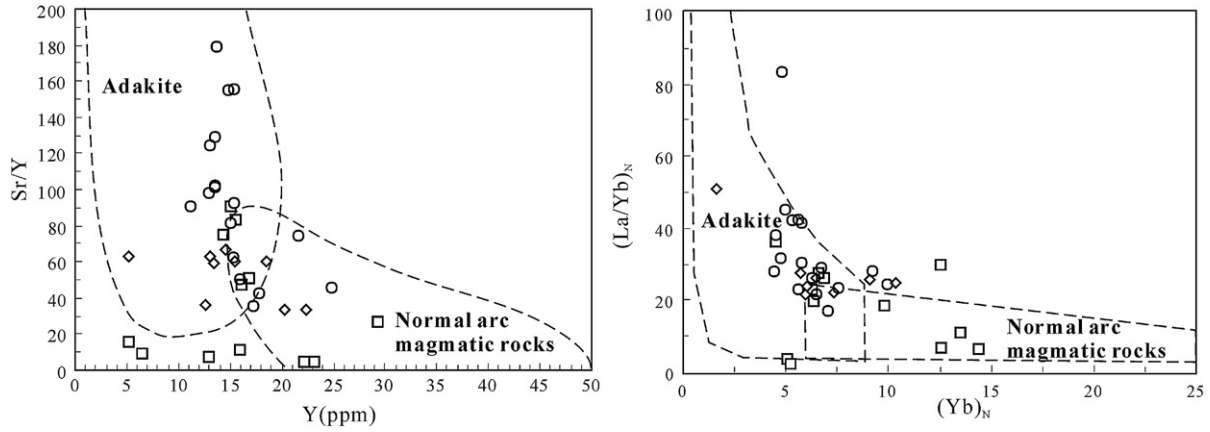

Fig. 9. Sr/Y versus Y and $(La/Yb)_N$ versus Yb_N diagram for Late Mesozoic granitoids (Defant and Drummond, 1990). Symbols and references are the same as in Fig. 2.

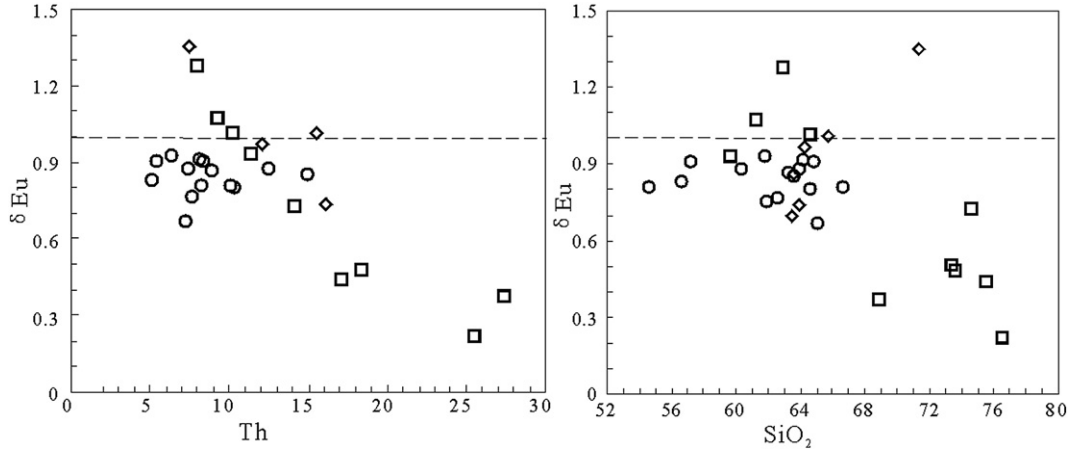

Fig. 10. Eu/Eu* versus Th and SiO_2 diagram for Late Mesozoic granitoids. Symbols and references are the same as in Fig. 2.

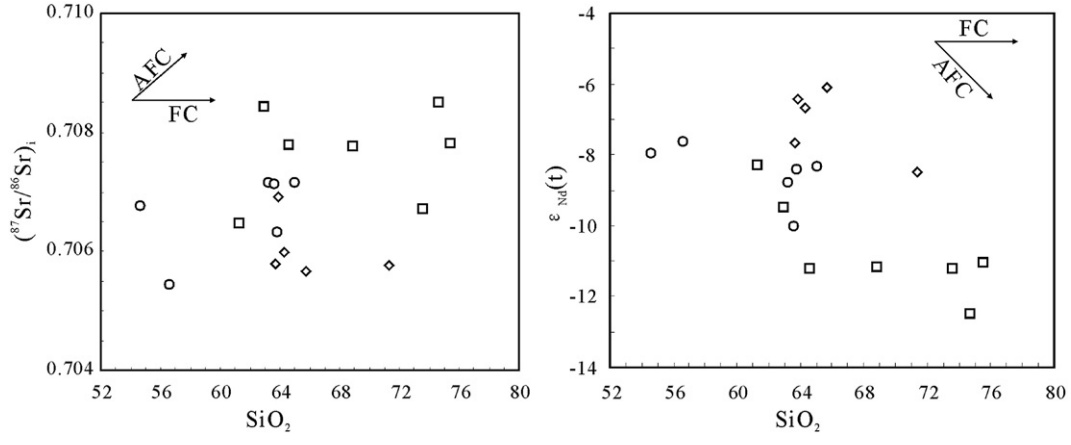

Fig. 11. $(^{87}Sr/^{86}Sr)_i$ and $\varepsilon_{Nd}(t)$ versus SiO_2 diagram for Late Mesozoic granitoids. FC: fractional crystallization; AFC: Assimilation–fractional crystallization. Symbols and references are the same as in Fig. 2.

the Mesozoic (Griffin et al., 1998). However, the timing and mechanism for lithospheric thinning underneath the North China and Yangtze Cratons remain poorly understood, in part owing to the lack of systematic studies on Late Mesozoic magmatism. Both geological features and published SHRIMP U–Pb zircon ages demonstrate that quartz diorite and monzonite intrusions are widespread in the southeastern Hubei Province, and these were emplaced earlier than other granitic rocks, such as the Tieshan granite (Mao et al., 1990; Shu et al., 1992; Zhou and Ren, 1994; Ma et al., 2005; Xue et al., 2006; Xie et al., 2006a). Experimental studies have demonstrated that the residual assemblages and melt compositions formed by partial melting of continental crust vary significantly with depth of melting. That is, granitic melts at pressures below 10 Kbar are characterized by significant negative Eu anomalies, low Sr/Y and (La/Yb)N ratios, and are in equilibrium with an anorthite-rich plagioclase residue, whereas granitic melts at pressures higher than about 15 Kbar show no significantly negative Eu anomalies, have high Sr/Y and (La/Yb)N ratios, and are in equilibrium with an garnet-rich residue, plus or minus albitic plagioclase (e.g. Defant and Drummond, 1990; Rapp and Watson, 1995; Patiño Douce and Beard, 1995). Thus, the geochemical characteristics of different stages of granitoid melt can be used to constrain the timing and mechanism for lithospheric thinning (Xu et al., 2007). As noted earlier, quartz diorite and monzonite in the southeastern Hubei show different geochemical characteristics, especially with regards to their Eu anomalies, and Sr/Y and (La/Yb)N ratios (Figs. 5, 9). Moreover, Nd–Sr isotopic evidence indicates that the quartz diorite from Echeng, Yangxin and Tieshan show closer affinities with an enriched mantle the Echeng granite (Table 2 and Fig. 7). Consequently, the magma responsible for the formation of the early stage quartz diorite and monzonite in the southeastern Hubei Province possibly originated from a somewhat deeper source than that of the later stage granite and granite porphyry. Thus, the integration of published SHRIMP zircon U–Pb ages with the changing compositional trends for the granitoids shown in this study indicates that lithospheric thinning probably commenced in the Early Cretaceous.

From the Late Mesozoic to Tertiary, isotopic compositions of mafic intrusive rocks and basalts from the MLYRB show a progressive change towards more depleted mantle characteristics, or a decreasing contribution of EM II mantle relative to DMM mantle (Chen et al., 2001). This temporal shift is similar to that seen in the Basin and Range Province, USA (DePaolo and Daley, 2000), which implies that lithospheric thinning commenced in the Late Mesozoic and terminated no later than the Tertiary (Xie et al., 2006c). Four recently obtained deep seismic reflection profiles in the MLYRB have revealed that a strongly-layered reflector exists at 20–30 km depth in the middle–lower crust, and this is possibly due to basaltic underplating and lithospheric thinning that occurred in the Late Mesozoic (see e.g. summary presented in Lu et al., 2005). Moreover, the thinning process was probably aided by upwelling of younger asthenospheric material due to subduction processes, replacing a part of old lithospheric mantle (Xu et al., 2000). Therefore, the lithospheric extensional regime that developed in the MLYRB during the Late Mesozoic was temporally associated with basaltic underplating, which led to lithospheric thinning and replacement during the early Cretaceous.

7. Conclusions

The combined geochemical and Sr–Nd isotopic analysis of the Late Mesozoic Yangxin, Tieshan and Echeng batholiths in the southeastern Hubei Province, MYLB, eastern China leads to the following conclusions:

(1) The Late Mesozoic granitoids consist predominatly of high-K and medium-K, calc-alkaline quartz diorite, monzonite and granite, are enriched in LREE and LILE, and the majority of them have high Sr, and low Y and Yb and thus are similar to high-SiO_2 adakites.

(2) Geological, geochemical and isotopic data preclude that these granitoids originated as direct the partial melts of a subducted slab or basaltic lower crust. Instead, these intrusions probably originated from partial melting of an enriched mantle source, followed by crustalassimilation and fractional crystallization of the parental magmas during magma ascent.

(3) Late Mesozoic granitoids in the southeastern Hubei, MYLB formed in an extensional setting. The integration of existing SHRIMP zircon U–Pb ages with the systematic compositional trends for these granitoids noted herein indicates that lithospheric thinning in the MYLB probably commenced in the Early Cretaceous.

Acknowledgements

We thank Zhang Zusong, Wei Shikun, Xiong Jizhuan, Li Xiangzhou, Yang Minyin and Zhou Shaodong for their kind help during field investigations. Song-Rong Li, Jia-Yi Feng, Jing Hu, Jin-Rong Li, Ji Qiu, Zhu-Yin Chu, Fu-Kun Chen are greatly appreciated for their assistance with the determination of major and trace elements, and Nd–Sr isotopic compositions. Many thanks to Dr. Castillo P and one anonymous reviewer for their helpful comments and suggestions. Thanks also to Eby N and Koole R for the editorial comments. This work was supported jointly by the National Science Foundation of China (40434011, 40402011), National Basic Research Program of China (2007CB41107, 2007CB41105), State Key Laboratory of Geological Processes and Mineral Resources, China University of Geosciences (GPM40504), China Postdoctoral Science Foundation and State Key Laboratory of Ore Deposit Geochemistry, Institute of Geochemistry, Chinese Academy of Sciences China (200402).

References

Atherton, M.P., Petford, N., 1993. Generation of sodium-rich magmas from newly underplated basaltic crust. Nature 362, 144–146.

Boynton, W.V., 1984. Cosmochemistry of the rare earth elements: meteorite studies. In: Henderson, P. (Ed.), Rare Earth Element Geochemistry. Elsevier, Amsterdam, pp. 63–114.

Castillo, P.R., 2006. An overview of adakite petrogenesis. Chinese Science Bulletin 51, 257–268.

Castillo, P.R., Janney, P.E., Solidum, R.U., 1999. Petrology and geochemistry of Camiguin Island, southern Philippines: insights to the source of adakites and other lavas in a complex arc setting. Contributions to Mineralogy and Petrology 134, 33–51.

Chang, Y.F., Liu, X.P., Wu, C.Y., 1991. The copper-iron belt of the lower and middle reaches of the Changjiang River. Geological Publishing House, Beijing, pp. 1–363 (in Chinese with English abstract).

Chen, J.-F., Yan, J., Xie, Z., Xu, X., Xing, F., 2001. Nd and Sr isotopic compositions of igneous rocks from the Lower Yangtze region in eastern China: constraints on sources. Physics and Chemistry of the Earth (A) 26, 719–731.

Defant, M.J., Drummond, M.S., 1990. Derivation of some modern arc magmas by melting of young subducted lithosphere. Nature 347, 662–665.

DePaolo, D.J., 1981. Trace element and isotopic effects of combined wall rock assimilation and fractional crystallization. Earth and Planetary Science Letters 53, 189–202.

DePaolo, D.J., Daley, E.E., 2000. Neodymium isotopes in basalts of the southwest basin and range and lithospheric thinning during continental extension. Chemical Geology 169, 157–185.

Gao, S., Zhang, B.-R., Jin, Z.-M., Hartmut, K., Luo, T.-C., Zhao, Z.-D., 1998. How mafic is the lower continental crust? Earth and Planetary Science Letters 161, 101–117.

Gao, S., Rudnick, R.L., Yuan, H.L., Liu, X.M., Liu, Y.S., Xu, W.L., Ling, W.L., Ayers, J., Wang, X.C., Wang, Q.H., 2004. Recycling lower continental crust in the North China craton. Nature 432, 892–897.

Griffin, W.L., Zhang, A., O'Reilly, S.Y., Ryan, C.G., 1998. Phanerozoic evolution of the lithosphere beneath the Sino-Korean Craton. In: Flower, M.F.J., Chung, S.L., Lo, C.H., Lee, T.Y. (Eds.), Mantle Dynamics and Plate Interaction in East Asia, Geodynamics Series, vol. 27, pp. 107–126.

Gutscher, M.-A., Maury, R., Eissen, J.-P., Bourdon, E., 2000. Can slab melting be caused by flat subduction? Geology 28, 535–538.

Hall, H.C., 1982. The importance and potential of mafic dyke swarm in studies of geodynamic process. Geosciences Canada 9, 145–154.

Irvine, T.N., Baragar, W.R.A., 1971. A guide to the chemical classification of the common volcanic rocks. Canadian Journal of Earth Science 8, 523–548.

Ishihara, S., 1977. The magnetite-series and ilmenite-series granitic rocks. Mining Geology 27, 293–305.

Jahn, B.-M., Wu, F.Y., Lo, C.-H., Tsai, C.-H., 1999. Crust–mantle interaction induced by deep subduction of the continental crust: geochemical and Sr–Nd isotopic evidence from post-collisional mafic–ultramafic intrusions of the northern Dabie complex, central China. Chemical Geology 157, 119–146.

Jiang, Y.-H., Jiang, S.-Y., Ling, H.F., Dai, B.-Z., 2006. Low-degree melting of a metasomatized mantle for the origin of Cenozoic Yulong monzogranite-porphyry, east Tibet: geochemical and Sr–Nd–Pb–Hf isotopic constraints. Earth and Planetary Science Letters 241, 617–633.

Li, X.H., 2000. Cretaceous magmatism and lithospheric extension in southeast China. Journal of Asian Earth Sciences 18, 293–305.

Lu, Q.T., Hou, Z.Q., Yang, Z.S., Shi, D.N., 2005. Underplating and dynamic evolution model in the lower Yangtze area: constraints from geophysical data. Science in China (D) 48, 985–999.

Ma, C.Q., Yang, K.G., Tang, Z.H., Li, Z.T., 1994. Magma-dynamics of Granitoids — Theory Method and a Case Study of the Eastern Hubei Granitoids. China. University of Geoscience Publishing Houses, Beijing, pp. 1–260 (in Chinese with English abstract).

Ma, C.Q., Li, J.W., Xu, H.J., Zhang, C., 2005. Late Mesozoic large igneous rocks: magma underplating and inplating. Petrology and Geodynamics Conference Abstracts in China, pp. 138–139 (in Chinese).

Macpherson, C.G., Dreher, S.T., Thirlwall, M.F., 2006. Adakites without slab melting: high pressure differentiation of island arc magma, Mindanao, the Philippines. Earth and Planetary Science Letters 243, 581–593.

Mao, J.R., Su, Y.X., Chen, S.Y., 1990. Intermediate-acid Intrusion in the Middle–Lower Reaches of Yangtze River and Relevant Mineralization. Geological Publishing House, Beijing, pp. 1–191 (in Chinese).

Mao, J.W., Wang, Y.T., Lehmann, B., Yu, J.J., Du, A.D., Mei, Y.X., Li, Y.F., Zang, W.S., Stein, H.J., Zhou, T.F., 2006. Molybdenite Re–Os and albite $^{40}Ar/^{39}Ar$ dating of Cu–Au–Mo and magnetite porphyry systems in the Yangtze River valley and metallogenic implications. Ore Geology Reviews 29, 307–324.

Martin, H., Smithies, R.H., Rapp, R., Moyen, J.-F., Champion, D., 2005. An overview of adakite, tonalite–trondhjemite–granodiorite (TTG), and sanukitoid: relationships and some implications for crustal evolution. Lithos 79, 1–24.

Menzies, M.A., Fan, W.M., Zhang, M., 1993. Palaeozoic and Cenozoic lithoprobes and the loss of >120 km of Archean lithosphere, Sino-Korean Craton, China. In: Prichard, H.M., et al. (Ed.), Magmatic Processes and Plate Tectonics. Geological Society of London, Special Publication, vol. 76, pp. 71–81.

Middlemost, E.A.K., 1994. Naming materials in the magma/igneous rock system. Earth Science Reviews 37, 215–224.

Pan, Y., Dong, P., 1999. The Lower Changjiang (Yangzi/Yangtze River) metallogenic belt, east China: intrusion-and wall rock-hosted Cu–Fe–Au, Mo, Zn, Pb, Ag deposits. Ore Geology Reviews 15, 177–242.

Patiño Douce, A.E., Beard, J.S., 1995. Dehydration-melting of biotite gneiss and quartz amphibolite from 3 to 15 Kbar. Journal of Petrology 36, 707–738.

Pei, R.F., Hong, D.W., 1995. The granites of South China and their metallogeny. Episodes 18, 77–86.

Qi, L., Grégoire, D.C., 2000. Determination of trace elements in twenty-six Chinese geochemistry reference materials by inductively coupled plasma-mass spectrometry. Geostandard Newsletter 24, 51–63.

Qian, Q., Chung, S.-L., Lee, T.-Y., Wen, D.-J., 2003. Mesozoic high-Ba–Sr granitoids from North China: geochemical characteristics and geological implications. Terra Nova 15, 272–278.

Rapp, R.P., Watson, E.B., 1995. Dehydration melting of metabasalt at 8–32 kbar: implications for continental growth and crust–mantle recycling. Journal of Petrology 36, 891–931.

Rock, N.M.S., Bowes, D.R., Wright, A.E., 1990. Lamprophyres. Glasgow and London, Blackie, pp. 1–156.

Rollinson, H.R., 1993. Using geochemical data: evaluation, presentation, interpretation. Longman Scientific and Technical, New York, pp. 1–352.

Shu, Q.A., Chen, P.L., Cheng, J.R., 1992. Geology of iron–copper deposits in Eastern Hubei Province, China. Ministry of Metallurgical Industry Publishing House, Beijing, pp. 1–532 (in Chinese).

Stein, H., Markey, R.J., Moegan, J.W., Hannah, J.L., Schersten, A., 2001. The remarkable Re–Os chronometer in molybdenite: How and why it works. Terra Nova 13, 479–486.

Sun, S.S., McDonough, W.F., 1989. Chemical and isotopic systematic basalt, implication for mantle composition and processes. Geological Society, Special Publication 42, 313–345.

Wang, Q., Zhao, Z.H., Bao, Z.W., Xu, J.F., Liu, W., Li, C.F., Bai, Z.H., Xiong, X.L., 2004. Geochemistry and petrogenesis of the Tongshankou and Yinzu adakitic intrusive rocks and the associated porphyry copper-molybdenum mineralization in southeast Hubei, East China. Resource Geology 54, 137–152.

Wang, Q., Wyman, D.A., Xu, J.-F., Zhao, Z.-H., Jian, P., Xiong, X.-L., Bao, Z.-W., Li, C.-F., Bai, Z.-H., 2006. Petrogenesis of Cretaceous adakitic and shoshonitic igneous rocks in the Luzong area, Anhui Province (eastern China): implications for geodynamics and Cu–Au mineralization. Lithos 89, 424–446.

Whalen, J.B., Currie, K.L., Chappell, B.W., 1987. A-type granites: geochemical characteristics, discrimination and petrogenesis. Contribution to Mineralogy and Petrology 95, 407–419.

Xiao, L., Clemens, J.D., 2007. Origin of potassic (C-type) adakite magmas: experimental and field constraints. Lithos 95, 399–414.

Xie, G.Q., Mao, J.W., Zhao, C.S., 2005a. Mineralizing pulses and geodynamic setting of Cu–Fe–Au polymetallic deposits in the Lower Yangtze valley, east-central China. In: Mao, J.W., Bierlein, F.P. (Eds.), Mineral Deposit Research. Meeting the Global Challenge. Springer, Berlin, pp. 1201–1204.

Xie, G.Q., Hu, R.Z., Mao, J.W., 2005b. Geological and geochemical characteristics of Early Cretaceous mafic dykes from North Jiangxi province and its geodynamics, China. Acta Geologica Sinica (English Edition) 79, 201–210.

Xie, G.Q., Mao, J.W., Li, L.L., Zhao, C.S., 2006a. Geological characteristics and mineral model of skarn Fe deposits from southeastern Hubei province. China. Mineral Deposits 25 (supp.), 147–150 (in Chinese with English abstract).

Xie, G.Q., Mao, J.W., Zhou, S.D., Ye, H.S., Yan, Q.R., Zhang, Z.S., 2006b. SHRIMP zircon U–Pb dating for volcanic rocks of the Dasi Formation in southeast Hubei Province, middle–lower reaches of the Yangtze River and its implications. Chinese Science Bulletin 51, 3000–3009.

Xie, G.Q., Mao, J.W., Hu, R.Z., Li, R.L., Cao, J.J., Jiang, G.H., Zhao, J.H., 2006c. Geochemical and Sr–Nd–Pb isotopic characteristics of Late Mesozoic mafic

dikes in Southern Jiangxi province, Southeast China: petrogenesis and tectonic implications. International Geology Review 48, 1023–1050.

Xie, G.Q., Mao, J.W., Li, R.L., Qu, W.J., Pirajno, F., Du, A.D., 2007. Re–Os molybdenite and Ar–Ar phlogopite dating of Cu–Fe–Au–Mo (W) deposits in southeastern Hubei, China. Mineralogy and Petrology 90, 249–270.

Xu, X., O'Reilly, S.Y., Griffin, W.L., Zhou, X., 2000. Genesis of youth lithospheric mantle in southeastern China: A LAM-ICPMS trace element study. Journal of Petrology 41, 111–148.

Xu, J.F., Shinjo, R., Defant, M.J., Wang, Q., Rapp, R.P., 2002. Origin of Mesozoic adakitic intrusive rocks in the Ningzhen area of east China: partial melting of delaminated lower continental crust? Geology 30, 1111–1114.

Xue, H.M., Dong, S.W., Jian, P., 2006. Mineral chemistry, geochemistry and U–Pb SHRIMP zircon data of the Yangxin monzonitic intrusive in the fore-land of the Dabie orogen. Science in China (D) 49, 684–695.

Xu, H.J., Ma, C.Q., Ye, K., 2007. Early cretaceous granitoids and their implications for the collapse of the Dabie orogen, eastern China: SHRIMP zircon U–Pb dating and geochemistry. Chemical Geology 240, 238–259.

Yan, J., Chen, J.-F., Xie, Z., Yang, G., Yu, G., Qian, H., 2005. Geochemistry of Late Mesozoic basalts from Kedoushan in the middle and lower Yangtze regions: constraints on characteristics and evolution of the lithospheric mantle. Geochimica 34, 455–469 (in Chinese with English abstract).

Zhai, Y.S., Yao, S.Z., Lin, X.D., Zhou, X.N., Wan, T.F., Jin, F.Q., Zhou, Z.G., 1992. Fe–Cu (Au) metallogeny of the Middle–Lower Changjiang region. Geological Publishing House, Beijing, pp. 1–235 (in Chinese).

Zhang, Q., Wang, Y., Qian, Q., Yang, J.H., Wang, Y.L., Zhao, T.P., Guo, G.J., 2001. The characteristics and tectonic-metallogenic significances of the adakites in Yanshan period from eastern China. Acta Petrologica Sinica 17, 236–2449 (in Chinese with English abstract).

Zhang, Q., Jian, P., Liu, D.Y., Wang, Y.L., Qian, Q., Wang, Y., Xue, H., 2003. SHRIMP dating of volcanic rocks from Ningwu area and its geological implications. Science in China (D) 46, 830–837.

Zhou, X.M., Sun, T., Shen, Z., Shu, L.S., Niu, Y.L., 2006. Petrogenesis of Mesozoic granitoids and volcanic rocks in South China: A response to tectonic evolution. Episodes 29, 26–33.

Zhou, X.R., Ren, J., 1994. Mesozoic Granites in the Middle–Lower Reaches of Yangtze River. Geological Publishing House, Beijing, pp. 1–119 (in Chinese).